Insights into uncertainties in future drought analysis using hydrological simulation model

Jin Hyuck Kim [1], Eun-Sung Chung[2*]

[1] Department of Civil Engineering, Chungnam National University, 99 Daehak-ro, Yuseong-gu, Daejeon 34134, South Korea.

[2] Faculty of Civil Engineering, Seoul National University of Science and Technology, 232 Gongneung-ro, Nowon-gu, Seoul 01811, South Korea.

[*]Corresponding author (eschung@seoultech.ac.kr)

Abstract

Hydrological analysis utilizing a hydrological model requires a parameter calibration process, which is largely influenced by the length of calibration data period and prevailing hydrological conditions. This study aimed to quantify these uncertainties in future runoff projection and hydrological drought based on future climate data and the calibration data of the hydrological model. Future climate data were sourced from three Shared Socioeconomic Pathway (SSP) scenarios (SSP2-4.5, SSP3-7.0, and SSP5-8.5) of 20 general circulation models (GCMs). The Soil and Water Assessment Tool (SWAT) was employed as the hydrological model, and hydrological conditions were determined using the Streamflow Drought Index (SDI), with calibration data lengths ranging from 1 to 20 years considered. Subsequently, the uncertainty was quantified using Analysis of Variance (ANOVA). After calibrating the SWAT parameters, the validation performance was found to be influenced by the hydrological conditions of the calibration data. Hydrological model parameters calibrated using a dry period simulated runoff with 11.4% higher performance in dry conditions and 6.1% higher performance in normal conditions, while hydrological model parameters calibrated using a wet period simulated runoff with 5.1% higher performance in wet conditions. The uncertainty contribution of the hydrological model in estimating future runoff was analyzed to be 3.9~9.8%, particularly significant in the low runoff period. The uncertainty contribution in future hydrological drought analysis resulting from the calibration of hydrological model parameters was analyzed to be 2.7% on average, which is lower than that of future runoff projection.

Key words: Future runoff, Hydrological drought, GCM, SWAT, Uncertainty

1. Introduction

In the current global climate scenarios, characterized by significant warming trends, there are increased challenges in understanding and managing water systems (IPCC, 2014; IPCC, 2021). Water availability for runoff is directly influenced by precipitation, while temperature affects water availability through its effect on evapotranspiration rates (Mahabadi and Delavar, 2024). These climatic changes significantly affect the availability of water resources and increase the occurrence and severity of hydrological extreme events such as floods and droughts in different regions (Milly et al., 2008; Santos et al., 2021). Hydrological projection is crucial for sustainable water resource planning and management (Peng et al., 2022; Yang et al., 2023; Yang et al., 2024). Consequently, quantifying the uncertainty in hydrological projection is essential as it directly affects the effectiveness of these management strategies and decision-making processes in ensuring the reliability and safety of water resources (Zhang et al., 2024).

Droughts, which could become more severe due to climate change, begin with a lack of precipitation and lead to a decrease in streamflow and soil moisture deficiency, encompassing a complex hydrological cycle that adversely affects plant and crop growth and human life. Generally, droughts progress over time into meteorological, agricultural, hydrological, and socio-economic droughts, and become a fatal disaster if prolonged (Sheffield and Wood, 2012). Consequently, future droughts due to climate change has been actively conducted, with most studies concluding that droughts are becoming more frequent and severe (Sung et al., 2018; Kim et al., 2021).

Hydrological drought requires an understanding of the hydrological cycle, including runoff, surface water, and groundwater. Runoff, a key indicator of hydrological drought, significantly affects the availability of water for agricultural, industrial, and domestic uses (Ghasemizade and Schirmer, 2013; Devia et al., 2015). Therefore, understanding and predicting runoff behavior is essential for hydrological drought analysis in water resource management and planning. While runoff data can be obtained from river observations within the region, there are limitations in observation technology and coverage. Consequently, simulated runoff data using regional meteorological data and hydrological models are utilized. Hydrological models simulate runoff by inputting meteorological data, soil data, and topographical data, allowing for the prediction of future hydrological cycles. However, these hydrological models are influenced by various factors, including the quality and quantity of input data, structural uncertainties of the models, and uncertainties in the calibration process (Xu et al., 2007; Renard

68 et al., 2010). Therefore, quantifying and recognizing these uncertainties is crucial to enhancing

69 the reliability of future hydrological analysis (Feng et al., 2019).

70 The future hydrological analyses considering uncertainty is essential for effective water

71 management. These projections are largely based on General Circulation Models (GCMs) and

72 hydrological models, which are critical tools for modelling the hydrological impacts of climate

73 change. However, GCMs introduce significant uncertainty in future runoff prediction due to

74 their inherent structural complexity and variability in scenario-based inputs (Broderick et al.,

75 2016). This uncertainty has a direct impact on the accuracy of runoff predictions and poses a

76 significant challenge to water resource management. The selection and use of GCMs have a

77 crucial role in shaping these uncertainties, making the consideration of a variety of GCMs and

78 shared socioeconomic pathways (SSP) scenarios essential for managing uncertainties and

79 improving projections (Vetter et al., 2015; Chae et al., 2024a). Indeed, Shi et al. (2022) had

80 shown how different evapotranspiration models embedded in GCMs affect runoff prediction,

81 highlighting GCMs and Representative Concentration Pathways (RCPs) as major factors

82 affecting uncertainty. Similarly, Lee et al. (2021a) had shown how the choice of GCMs

83 significantly affects prediction of water storage in wetlands under future climate scenarios. To

84 understand these uncertainties, Wang et al. (2020) suggested the use of a broad ensemble of at

85 least 10 GCMs, which allowed for a more comprehensive assessment of hydrological impacts

86 and helped to reduce the inherent uncertainties associated with climate change. Thus, the use

87 of a wide range of GCMs is an essential strategy for maximizing the effectiveness of water

88 resource management under global climate change conditions.

89 The hydrological model calibration involves significant uncertainty, especially when

90 predicting future conditions. This process, crucial for aligning model parameters with historical

91 data, often incorrectly assumes that parameters validated under past hydrological conditions

92 will remain valid in the future. Thirel et al. (2015) and Fowler et al. (2016) demonstrated that

93 models calibrated with historical climate data might not perform accurately under changed

94 conditions, leading to substantial uncertainties in runoff projections. This challenge is

95 exacerbated by the dependency of model parameters on the hydrological conditions prevalent

96 during the calibration period (Merz et al., 2011; Coron et al., 2012). Effective calibration

97 strategies, therefore, must consider variable climate scenarios to ensure model robustness. This

98 involves rigorous calibration under diverse conditions to validate hydrological models'

99 reliability in projecting future water resource availability (Saft et al., 2016; Dakhlaoui et al.,

100 2017). Furthermore, the interaction between model parameters and hydrological conditions

during these periods often complicates the calibration process, underscoring the need for robust validation techniques. The duration of the calibration period also contributes significantly to the uncertainty in runoff projection. Razavi and Tolson (2013) and Arsenault et al. (2018) highlighted the importance of sufficiently long calibration periods to ensure meaningful calibration and validation results. In addition, Kim et al. (2011) cautioned against using overly short calibration periods, as this can lead to large and unstable model performance variability during calibration and validation. Despite the emphasis on longer calibration periods, Perrin et al. (2007), Sun et al. (2017), Yu et al. (2023), and Ziarh et al. (2024) had found that an extended calibration data length does not guarantee improved model performance, suggesting a nuanced approach to calibration period selection. These insights underlined the complex interplay among calibration length, model parameter selection, and climatic variability in shaping the reliability of hydrological models.

The rigorous quantification of uncertainties in hydrological modeling is essential to enhance the reliability of water resources planning and management. This study employs Analysis of Variance (ANOVA), a statistical method widely used in hydrological studies, to systematically quantify uncertainties in hydrological projections. ANOVA dissects the variance observed in projections into contributions from various sources of uncertainty, such as GCM outputs, SSP scenarios, and hydrological model parameters (Qi et al., 2016; Chae et al., 2024b). By identifying the dominant sources of variability and analyzing their interactions, ANOVA provides a clear understanding of how different factors drive uncertainties in hydrological projections. Recent applications of ANOVA in future hydrological studies demonstrated its effectiveness in understanding model-driven uncertainties (Chen et al., 2022; Yuan et al., 2022; Mo et al., 2024).

This study focuses on the uncertainty in future hydrological analyses, which are influenced by hydrological model parameters during different calibration periods under future climate data and different hydrological conditions. This research utilizes the Soil and Water Assessment Tool (SWAT), a widely recognized hydrological model, to analyze the impact of hydrological conditions during the calibration period on the projection of future runoff and hydrological drought. Three SSP scenarios and 20 GCMs were used to consider uncertainty due to future climate, and different hydrological conditions according to the Streamflow Drought Index (SDI) and different calibration period data lengths from 1 to 20 years were used to consider uncertainty in hydrological model parameter calibration. This study aims to contribute to the

133   refinement of hydrological modelling practices by quantifying the uncertainties associated with

134   future runoff projection and hydrological drought analysis.

135   This manuscript is structured as follows. In Section 2, the study area, datasets, and the

136   methodologies used in this study are described, including the SWAT model, the ANOVA

137   framework, and the statistical validation procedures. In Section 3, the results of the analysis

138   are presented, showing the effects of calibration conditions on model performance and

139   quantifying the uncertainty contributions from various sources for both future runoff and

140   hydrological drought. In Section 4, the implications of these findings are discussed in the

141   context of previous research. Finally, Section 5 summarizes the main conclusions of this study.

142

2. Methodology

2.1 Procedure

145   The procedure of the study is as follows. First, topographic data for four dam basins in South

146   Korea were established, taking into account the overall hydrological characteristics of the

147   region, and observed dam inflow data were utilized to consider the length and hydrological

148   conditions of the hydrological model calibration data. The length of the calibration data

149   considered ranged from 1 to 20 years, and hydrological conditions were categorized using the

150   Streamflow Drought Index (SDI). Subsequently, validation performance analysis was

151   conducted, with calculations varying according to the length of calibration data and

152   hydrological conditions (Dry, Normal, and Wet). For the study, future climate data from 20

153   Coupled Model Intercomparison Project Phase 6 (CMIP6) GCMs and three SSP scenarios

154   (SSP2-4.5, SSP3-7.0, and SSP5-8.5) were bias-corrected. Future runoff projection and

155   hydrological drought were then analyzed using calibrated hydrological model parameters under

156   different conditions along with the future climate data. Finally, the uncertainties in the future

157   hydrological analysis were quantified using the Analysis of Variance (ANOVA).

158

2.2 Study area and datasets

160   The study areas selected in this study are the Andong (AD), Chungju (CJ), Habcheon (HC),

161   and Seomjingang (SJ) dam basins located in Korea as shown in Fig. 1. To achieve stable

162   calibration and validation results for a hydrological model, it is imperative to choose

163 catchments with extensive hydrological data records. This enables the accurate estimation of
164 appropriate calibration data lengths through various testing periods of the hydrological model.
165 Furthermore, incorporating a variety of basins is crucial to ensure that the findings of this study
166 are not biased by specific hydrological conditions. These four basins, which have the longest
167 hydrological records in Korea, are situated in major river basins as shown in Table S1: AD
168 (1,584 km²) and HC (925 km²) in the southeastern Nakdong River basin, CJ (6,648 km²) in the
169 southern Han River basin, and SJ (763 km²) in the southwestern Seomjin River basin. These
170 regions are devoid of artificial structures, ensuring that runoff remains natural and unaltered.
171 Located in different regions of Korea, these basins have a range of hydrological conditions and
172 runoff characteristics, providing a representative cross-section of the country's hydrological
173 characteristics.

174

175 **2.3 Soil and water assessment tool (SWAT)**

176 The SWAT was used to calibrate hydrological processes in our study basin. The SWAT is
177 particularly adept at simulating runoff and other hydrological variables under a wide range of
178 environmental conditions and is a robust, physically based, semi-distributed model. Its
179 efficiency in modelling hydrological cycles within basins relies on simple input variables to
180 produce detailed hydrological outputs. The capability of this model has been effectively shown
181 in various studies, including those in South Korea (Kim et al., 2022; Song et al., 2022).

182 The core of the SWAT model is the water balance equation, which integrates daily weather
183 data with land surface parameters to calculate water storage changes over time:

184

185 $$SW_t = SW_0 + \sum_{i=0}^{t}\left(R_{day} - Q_{surf} - E_a - w_{seep} - Q_{gw}\right) \qquad (1)$$

186

187 where SW_0 is the initial soil moisture content (mm), SW_t is the total soil moisture per day
188 (mm), R_{day} is precipitation (mm), Q_{surf} is surface runoff (mm), E_a is evapotranspiration
189 (mm), W_{seed} is penetration, Q_{gw} is groundwater runoff (mm), and t is time (day).

190 For rainfall-runoff analysis, the SWAT model is structured into several sub-basins, each of
191 which is further subdivided into Hydrologic Response Units (HRUs) based on different soil
192 types, land use and topography. Each HRU independently simulates parts of the hydrological

cycle, allowing a granular analysis of basin hydrology. This setup reflects the spatial heterogeneity within the basin and allows continuous simulation of hydrological processes over long time periods, enhancing the utility of the model for climate change studies. The model was calibrated and validated using R-SWAT for parameter optimization. R-SWAT incorporates the SUFI-2 algorithm, which is known for its rapid execution and precision in parameter optimization, ensuring accurate and reliable simulation results (Nguyen et al., 2022). In this study, the setup and evaluation of the SWAT model for the historical period were performed using observed data. The model was forced with observed meteorological data, and the parameters were calibrated and validated against historical daily dam inflow records for the period 1980-2023.

2.4 Streamflow drought index (SDI)

The drought index was used to classify hydrological conditions considering the calibration effect of periods with different hydrological conditions. SDI is a commonly used method for quantifying the severity and duration of drought conditions in a river basin. It is based on the comparison of observed streamflow with a historical reference period, usually the average streamflow over a long-term period. SDI which is a hydrological drought index, is calculated as Eq. 2. (Nalbantis and Tsakiris, 2009).

$$SDI_{i,k} = \frac{V_{i,k} - \bar{V}_k}{S_k} \tag{2}$$

where $V_{i,k}$ is the runoff accumulated during the kth period in the ith year, and $\bar{V}_k$ and S_k represent the average and standard deviation of the accumulated river flow, respectively.

The critical level is mainly the average $\bar{V}_k$. In small scale rivers, the runoff rate approximates the Log-normal distribution type and the probability distribution type is distorted. Therefore, the runoff rate must be converted to fit the normal distribution. When converting to a two-variable log-normal distribution type, SDI is finally equal to Eq, 3, and $y_{i,k}$ is a value obtained by taking the natural logarithm of the amount of river water, such as Eq. 4.

$$SDI_{i,k} = \frac{y_{i,k} - \bar{y}_k}{S_{y,k}}, i = 1,2,\cdots, k = 1,2,3,4 \tag{3}$$

$$y_{i,k} = \ln(V_{i,k}), I = 1,2,\cdots, K = 1,2,3,4 \tag{4}$$

To classify the hydrological conditions, this study categorized -0.5 and below as Dry, 0.5 and above as Wet, and -0.5 to 0.5 as Normal (Nalbantis and Tsakiris, 2009; Hong et al., 2015).

2.5 General Circulation Models (GCMs)

In this study, M1 to M20 GCMs from the CMIP6 suite that have been consistently used in studies for East Asia and Korea were selected for future runoff projection and hydrological drought analysis. The details of the development institutions, model names and resolutions of these 20 GCMs were presented in Table S2.

The climate data from the GCMs were evaluated using daily observed climate data provided by the Korea Meteorological Administration (KMA). The evaluation used observed data from the past period (1985-2014) to evaluate the future climate data from the GCMs, which were analyzed for two future periods: the near future (NF) and the distance future (DF). The future climate change scenarios used were SSP2-4.5, SSP3-7.0 and SSP5-8.5. The SSP scenarios are divided into five pathways based on radiative forcing, reflecting different levels of future mitigation and adaptation efforts (O'Neill et al., 2016). The SSPs are numbered from SSP1 to SSP5, with SSP1 representing a sustainable green pathway and SSP5 representing fossil fuel driven development. The numbers 4.5 to 8.5 indicate the level of radiative forcing (4.5: 4.5 W m-2, 7.0: 7.0 W m-2 and 8.5: 8.5 W m-2). For the analysis of future changes, the calibrated SWAT model was then driven by bias-corrected future climate projection data from the 20 GCMs under the three SSP scenarios. This approach ensures that the model's baseline performance is grounded in observational data, while the future analysis specifically assesses the uncertainties propagated from the climate projections and hydrological modeling choices.

2.6 Bias correction using quantile mapping

The GCMs data outputs in a gridded format with a fixed resolution, requiring the use of spatial interpolation methods. In this study, the inverse distance weighting (IDW) method was employed to spatially interpolate the GCM data based on the locations of the Korea Meteorological stations. Subsequently, to align the GCM data with the actual observational data, the quantile mapping method was utilized. This method adjusts the GCM data based on the quantile relationship between the cumulative distribution functions (cdf) of the GCM data and the observed data (Gudmundsson et al., 2012). The quantile mapping method is described by Eq (5).

$$P_o = F_o^{-1}\big(F_m(P_m)\big) \tag{5}$$

where, P_o and P_m represent observed and simulated climate variables, F_m is the CDF of P_m and F_o^{-1} is the inverse CDF corresponding to P_o.

The quantile relationship can be also derived directly using parametric transformations. In this study, the linear method of parametric transformation was adopted as Eq. (6).

$$\hat{P} = a + bP_m \tag{6}$$

where, $\hat{P}$ represents the best estimate of P_o and a and b are free parameters that are subject to calibration.

2.7 Quantifying uncertainty

The ANOVA used in this study is an effective statistical method that decomposes the total sum of squares (SST) into contributions from different sources and their interactions. This method would be particularly useful in the study framework, as it allows us to assess not only the individual effects of each source of uncertainty but also the combined effects of these sources interacting with each other (Bosshard et al., 2013; Lee et al., 2021a).

277 For this analysis, the primary sources of uncertainty considered are General Circulation Models
278 (GCMs), Shared Socioeconomic Pathway (SSP) scenarios, hydrological conditions (HC)
279 during the calibration period, and period length (PL). Each of these sources could have a
280 significant impact on the projections of hydrological models; therefore, their comprehensive
281 evaluation is crucial (Morim et al., 2019; Yip et al., 2011). Higher-order interactions (e.g.,
282 three-way) were excluded as they are often difficult to interpret physically and can introduce
283 noise into the model.

284

285 $$SST = SS_{GCMs} + SS_{SSPs} + SS_{HC} + SS_{PL} + SS_{Interactions(2-way)} + SS_{Residuals} \qquad (7)$$

286

287 where each term (SS) indicates the sum of squares attributed to each factor or interaction.
288 Here, SS_{GCMs}, SS_{SSPs}, SS_{HC}, and SS_{PL} represent the sum of squares due to GCMs, SSPs, HC,
289 and PL, respectively, known as the main effects. The remaining terms represent the sum of
290 squares due to the interactions among GCMs, SSPs, hydrological conditions, period length,
291 their two-way interactions, and the residual error.

292 The model setup for ANOVA considered 20 GCMs, three SSP scenarios, three hydrological
293 conditions, and different calibration period lengths. This resulted in a total of 120 unique
294 combinations for each basin analyzed. Initially, the SST, representing the total variation within
295 the data, was calculated. Subsequently, the sum of squares attributable to each source of
296 uncertainty was computed. To quantify the relative impact of each source, its contribution was
297 calculated as the proportion of its Sum of Squares relative to the Total Sum of Squares. This
298 provides a clear measure of the percentage of total uncertainty explained by each factor and
299 interaction.

300 The statistical robustness and validity of the ANOVA models were rigorously evaluated. First,
301 the overall goodness-of-fit for each model was assessed using the Adjusted R-squared (R^2_{adj}),
302 defined as Eq. (8).

303

304 $$R^2_{adj} = 1 - \frac{(1-R^2)(n-1)}{n-k-1} \qquad (8)$$

305

306 Where, R^2 is the coefficient of determination, n is the number of observations, and k is the

307 number of predictions. This metric is preferred over the Standard R-squared as it adjusts for

308 the number of predictors in the model, providing a more accurate measure of model fit.

309 Second, a residual analysis was conducted to verify that the core assumptions of ANOVA were

310 met. The normality of residuals was a primary focus of this validation, examined both

311 statistically with the Shapiro-Wilk test and visually using Quantile-Quantile (Q-Q) plots. The

312 Shapiro-Wilk test evaluates the null hypothesis that the residuals are normally distributed.

313 However, given the large sample size in this study, which can lead to statistically significant

314 results even for minor deviations from normality, greater emphasis was placed on the visual

315 inspection of Q-Q plots to assess practical adherence to the normality assumption. The

316 assumption of homoscedasticity (constant variance of residuals) was also inspected using

317 Residuals vs. Fitted values plots. These validation steps ensure that the results of the

318 uncertainty partitioning are statistically sound and reliable. All statistical analyses were

319 performed using the R software environment.

320

321 **3. Results**

322 **3.1 Determining the hydrological conditions**

323 The calculated SDI was shown in Fig. S. 1. The SDI values of AD and HC in the Nakdong

324 River basin showed drought conditions similar to the actual events that occurred in 1994-1995,

325 2009, 2014-2015, 2016, 2017 and 2022 (Karunakalage et al., 2024). Similarly, SDI values of

326 CJ in the Han River basin accurately reflected the actual drought events of 2014-2015 and 2017

327 (Lee et al., 2021b). Finally, those of SJ in the Seomjin River basin also represented the drought

328 events of 1995, 2005-2006 and 2018-2019, demonstrating that the SDI was accurately

329 calculated. Therefore, this study using the observed inflow data of the four basins could reflect

330 the hydrological drought characteristics of the historical periods in South Korea.

331

332 **3.2 SWAT parameter calibration**

333 The simulated runoff data were analyzed for performance using the Kling-Gupta Efficiency

334 (KGE; Gupta et al., 2009). KGE was developed to overcome some limitations of the commonly

335 used Nash-Sutcliffe Efficiency (NSE) in performance analysis (Gupta et al., 2009). The

336 attributes of KGE include focusing on a few basic required properties of any model simulation:

337   (i) bias in the mean, (ii) bias in the variability, and (iii) cross-correlation with the observational

338   data (measuring differences in hydrograph shape and timing). The parameter optimization of

339   SWAT was performed as shown in Fig. S. 2, considering the data length of the calibration

340   period from 1 to 20 years. A rigorous validation scheme was adopted to prevent bias from

341   specific period characteristics and to ensure a robust evaluation of predictive performance. For

342   any given calibration period, the validation was not performed on the entire remaining period

343   as a single dataset. Instead, we conducted a year-by-year validation, calculating a separate KGE

344   value for each individual year not included in the calibration set. For instance, if a model was

345   calibrated on years 1-5 from a 20-year record, 15 distinct single-year KGE values were

346   calculated for years 6 through 20. This approach strictly separates calibration and validation

347   datasets and ensures that model performance is assessed across a diverse range of annual

348   hydrological conditions, providing a robust foundation for the subsequent uncertainty analysis.

349   Following parameter optimization, KGE values as shown in Fig. 2 were found to be suitable

350   for conducting the study, with all four dam basins achieving values above 0.60. The

351   performance improvements are as follows: AD's KGE increased from 0.55 before calibration

352   to 0.64 after calibration, CJ's from 0.68 to 0.75, HC's from 0.70 to 0.80, and SJ's from 0.50 to

353   0.73. This improvement in KGE after calibration underscores the robustness of the

354   hydrological models used and their enhanced capability in projecting future runoff.

355

356   **3.3 Effect of varying data length**

357   The validation performance according to the calibration data length was shown in Fig. 3. The

358   impact of calibration data length on validation performance was analyzed, revealing a departure

359   from previous studies, which suggested that longer calibration data lengths lead to more

360   effective optimization of hydrological model parameters. Instead, the influence of calibration

361   data length on performance is all different by basin. For AD, the best performance was

362   observed with a 2-year period, averaging a KGE of 0.66, while the 1-year period resulted in

363   the lowest performance with an average KGE of 0.48. The Inter Quartile Range (IQR) showed

364   that variations were smaller for periods longer than 10 years (average IQR of 0.15) compared

365   to those less than 10 years (average IQR of 0.20). For CJ, the optimal performance was at a 15-

366   year period with an average KGE of 0.72, and the lowest at a 4-year period with an average

367   KGE of 0.58. The IQR values were 0.19 for periods under 10 years and 0.20 for periods over

368   10 years, indicating minor differences due to length. For HC, the highest KGE of 0.77 was

369   recorded at 19 years, and the lowest KGE of 0.66 at 1 year. The IQR for periods under 10 years

370   was 0.19, and 0.10 for those over 10 years, showing that longer periods yielded less variability.

371   In the case of SJ, a 9-year period had a KGE of 0.68, and a 20-year period had a KGE of 0.60,

372   with IQRs of 0.23 for periods under 10 years and 0.21 for those over. While the best validation

373   performance due to calibration data length varied by basin, it was observed that the differences

374   due to the period decrease as the length increases.

375

3.4 Effect of varying hydrological conditions

377   The performance analyses based on the hydrological conditions of the calibration and

378   validation periods are shown in Fig. S. 3 and Table 1. Fig. S. 3 shows the KGE values and the

379   confidence level (prediction) for each hydrological condition during the validation period

380   according to the SDI values. Overall, during the dry and normal validation periods, it was

381   analyzed that lower SDI values (dry condition) correlated with higher KGE values. This

382   indicates that SWAT parameters calibrated with dry validation period data effectively simulate

383   runoff under Dry and Normal hydrological conditions. For wet validation periods, higher SDI

384   values (wet condition) correlate with higher KGE values, indicating that SWAT parameters

385   calibrated with wet calibration period data accurately simulate runoff under wet conditions.

386   As shown in Table 1, the average KGE according to hydrological conditions is as follows. The

387   KGE values for each dam basin, according to the hydrological conditions of the calibration-

388   validation periods, are as follows: For AD, D-D (Dry-Dry; hydrological conditions for

389   calibration and validation periods, respectively) was 0.480, higher than W-D (Wet-Dry) of

390   0.382; D-N (Dry-Normal) was 0.573, higher than W-N (Wet-Normal) of 0.510; and W-W

391   (Wet-Wet) was 0.642, higher than D-W (Dry-Wet) of 0.571. For CJ, D-D was 0.743, higher

392   than W-D at 0.725; D-N was 0.643, higher than W-N at 0.615; and W-W was 0.706, higher

393   than D-W at 0.674. For HC, D-D was 0.732, higher than W-D at 0.670; D-N was 0.738, higher

394   than W-N at 0.714; and W-W was 0.769, higher than N-W (Normal-Wet) at 0.757. Lastly, for

395   SJ, D-D was 0.557, higher than W-D at 0.515; D-N was 0.677, higher than W-N at 0.650; and

396   W-W was 0.684, higher than D-W at 0.674.

397   The performance evaluation classified by data length and hydrological conditions for validation

398   are influenced by hydrological conditions for calibration, but the optimal data length for the

399   best performance varies between basins as shown in Fig. 4. These results confirm the

400   importance of uncertainty in hydrological models due to differences in hydrological conditions

during the calibration and validation periods, as suggested by previous studies (Bai et al., 2022; Fowler et al., 2016). Furthermore, the different data lengths with high validation performance for each basin confirm the opinion that shorter calibration data lengths can be applied under limited data conditions (Perrin et al., 2007; Yu et al., 2023), instead of the traditional opinion that longer calibration data lengths are better for hydrological modelling (Arsenault et al., 2018; Kim et al., 2011).

3.5 Bias correction for GCMs

In this study, climate data from GCMs were bias-corrected using observed climate data from KMA weather stations located within each dam basin. Fig. S. 4 describes the root mean square error (RMSE), Pearson coefficient and standard deviation (SD) in a Taylor diagram. After bias correction, all GCMs' climate data showed improved performance. The Pearson coefficient of precipitation increased from 0.04 to 0.99 and the RMSE decreased from 4.43 to 0.05. Similarly, the Pearson coefficients of the daily maximum and minimum temperatures averaged 1.00 and their RMSEs averaged 0.08. This is an indication that the GCM's climate data after bias correction were appropriate for use in this study.

3.6 Projection of climate variable

The future climate data from bias-corrected GCMs were depicted in Fig. 5 and Table S3. The future period was divided into NF and FF, and it was found that daily precipitation, maximum temperature, and minimum temperature all increased overall. Except for July and August, future precipitation generally increased, with significant rises particularly noted in April and May. In NF, the largest increase occurred in May under SSP2-4.5 with 51.4 mm, while in DF, the largest increase occurred in April under SSP5-8.5 with 59.8 mm. The largest decrease in NF was calculated for July under SSP5-8.5, and in DF it was most significant under SSP3-7.0, indicating considerable uncertainties in the GCMs during July and August, the months of the highest precipitation.

With regard to maximum temperatures, the analysis shows that there has been an increase in all months except April in NF, especially in fall (September-November). This increase was more pronounced in the DF than in the NF, with the largest increases observed under SSP5-8.5. Similarly, the minimum temperature was found to have increased in the future compared to the past, following the same trend as the maximum temperature.

433

3.7 Projection future runoff

3.7.1 Annual runoff change

The future runoff was projected using climate data and hydrological model parameters as shown in Fig. S. 5. Overall, future runoff is expected to increase relative to the historical data, with more significant increases projected during DF than NF As the SSPs change (e.g. from SSP2-4.5 and SSP3-7.0 to SSP5-8.5), not all annual runoff show a consistent increase with the scenario change, as shown in Table 2. In particular, the increase in annual runoff under SSP5-8.5 was not always higher than SSP2-4.5 or SSP3-7.0. These differences were analyzed to vary significantly between different basins and GCMs.

For AD, the future seasonal runoff is likely to increase in all seasons except summer. This increase would be more pronounced during DF than NF, with the largest increases occurring under SSP5-8.5. For CJ, the future runoff is expected to increase compared to the past in all seasons, with the highest increase observed in DF under SSP3-7.0 and the lowest increase under SSP5-8.5. For HC, future runoff is expected to increase in all seasons except fall, with the greatest variability in fall under SSP3-7.0. For SJ, future runoff is projected to increase compared to the past in all scenarios except NF under SSP3-7.0.

450

3.7.2 Differences in projected future runoff due to hydrological model parameters

The future runoff projections using many calibrated sets of hydrological model parameters were analyzed using the flow duration curve (FDC). In water resources planning and drought management, the differences in future runoff projections due to hydrological model parameters at low runoff are critical. These differences are shown in Fig. S. 6, and the differences in Q75 for each basin and their proportions relative to the mean runoff are shown in Table 3. The basin with the largest differences due to hydrological conditions in the calibration period was analysed as HC. HC is a basin with relatively low precipitation and a small watershed area. CJ, the largest basin, was analysed to have a 5-6% difference in runoff by hydrological model parameters, which means that the effect of hydrological model calibration is larger in smaller basins. The overall trend shows larger variances in DF than NF, and these variances were more pronounced for SSP5-8.5 scenario than SSP2-4.5. This indicates the need to consider the variations caused by hydrological model parameters when managing water resources during

464   both flood and drought periods. Table S4 details the top three GCMs that showed the most
465   significant differences in runoff projections due to hydrological model parameters for each
466   basin. Models, M5 and M6 were consistently identified as having the largest discrepancies in
467   future runoff projections due to hydrological model parameters.

468

469   **3.8 Uncertainty contribution of future runoff projections**
470   3.8.1 Statistical significance of ANOVA results for future runoff projection
471   Before assessing the significance of individual uncertainty sources, the statistical validity of
472   the developed ANOVA models was confirmed. The goodness-of-fit for all monthly models
473   across all four basins and both future periods (NF and DF) were exceptionally high, with
474   Adjusted R-squared values consistently exceeding 0.99. This indicates that the selected factors
475   and their two-way interactions explain more than 99% of the variance in the projected future
476   runoff. Furthermore, a comprehensive residual analysis was conducted for each model. While
477   statistical tests for normality, such as the Shapiro-Wilk test, are sensitive to large sample sizes,
478   the visual inspection of Q-Q plots and Residuals vs. Fitted plots confirmed that the assumptions
479   of normality and homoscedasticity were practically satisfied, ensuring the reliability of the
480   subsequent significance testing (Fig. S. 7-8).

481   The factors related to the hydrological model calibration, HC and PL, were also found to be
482   statistically significant for the future runoff projections. Table 4-5 summarizes the frequency
483   of statistical significance ($p < 0.05$) for each factor across the four study basins. The values
484   indicate the number of basins out of four where the factor was found to be significant. Although
485   their influence was smaller than that of GCMs and SSPs, both HC and PL were significant (p
486   < 0.05) in numerous months, particularly during the low-flow periods such as spring and winter.
487   This result highlights that the calibration conditions should be considered an important source
488   of uncertainty.

489   Among the two-way interactions, the GCM:SSP interaction consistently showed the highest
490   statistical significance ($p < 0.001$) across all months and basins, indicating that the effect of a
491   GCM is strongly dependent on the chosen SSP scenario, and vice versa. Furthermore,
492   interactions involving the calibration factors, such as GCM:HC and HC:PL, were also found
493   to be statistically significant in various months. This finding is crucial as it demonstrates that
494   the uncertainty stemming from hydrological model calibration does not act in isolation but

interacts in a complex manner with future climate projections, thereby influencing the overall uncertainty of future runoff.

3.8.2 Contribution of uncertainty using the ANOVA

Fig. S. 9 shows the relative contributions of different factors to the uncertainties in future runoff projections for each basin. Fig. 6 specifically highlights the uncertainty contributions attributed to hydrological models. The differences in future climate data from the GCMs were found to be the largest source of uncertainty, contributing over 60%. This is more significant during NF than DF, due to the increased climate variability in GCM projections during the NF, as discussed in Section 3.6.

The uncertainty contributions from hydrological models were most significant during the spring (Mar-May) and winter (Dec-Feb) periods, as shown in Table S5. The results of the analysis for each basin were as follows: For AD, the hydrological model uncertainty was most significant in spring (NF: 7.54%, and DF: 5.86%), with a maximum of 9.76% in June for NF and 7.54% in April for DF. In CJ, the highest uncertainties were also found for NF in winter (3.9%) and for DF in spring (3.96%). HC showed the highest uncertainty in winter (NF: 6.09%, and DF: 5.5%), with a maximum in November (NF: 9.76%, and DF: 8.92%). For SJ, the most significant contributions were found in spring (NF: 5.58%, and DF: 3.88%). In the end, hydrological model uncertainties were more significant in months with lower runoff.

3.9 Future hydrological drought uncertainty

3.9.1 Future hydrological drought uncertainty according to hydrological conditions

To quantify the uncertainty in the future hydrological drought analysis using the calibrated sets of hydrological model parameters, the Streamflow Drought Index (SDI) was used to calculate the hydrological drought conditions during the future period. For the uncertainty analysis, runoff data were considered for both historical and future periods. Table 6 shows the difference in the number of drought events under hydrological conditions during the calibration period after calculating SDIs for 3-month, 6-month, and 12-month durations. The difference in the number of drought events according to the hydrological conditions of the calibration period was analysed differently for each SSP and basin. The difference was significant for the shorter duration of 3 months.

According to the analysis by basin, the difference in the number of drought events in the AD basin with a 3-month duration was calculated to be the largest, with an average of 4.93 events, followed by SJ, CJ, and HC. Between the near future (NF) and distant future (DF), the difference in the number of drought events under the overall hydrological conditions was larger in the NF, and this difference was calculated differently by basin, confirming the need for basin-specific analysis in water resource management planning. Therefore, the uncertainty quantification of the drought analysis was performed using the SDI with a duration of 3 months.

3.9.2 Statistical significance of ANOVA results for future hydrological drought

To confirm the statistical validity of the ANOVA models for the future hydrological drought analysis, the goodness-of-fit was evaluated. The models showed a high goodness-of-fit, with Adjusted R-squared values consistently greater than 0.99 for all annual models across the four basins. This indicates that the selected factors and their two-way interactions explain more than 99% of the variance in the future drought projections, ensuring the reliability of the analysis.

Table 7 summarizes the frequency of statistical significance ($p < 0.05$) for each factor, aggregated by decade, to provide a concise overview of the results across the entire future period. The values indicate the number of basins (out of four) where the factor was found to be significant for the majority of years within that decade. The primary climate-related factors, GCM and SSP, were consistently identified as the most significant sources of uncertainty. As shown in Table 7, both factors were found to be highly significant across all four basins for all decades, underscoring the profound impact of climate model choice and emission scenarios on drought projections.

The hydrological model calibration factors, HC and PL, also proved to be important sources of uncertainty. Both factors were statistically significant across all four basins for the entire future period. This finding reinforces that the hydrological conditions and data length used for model calibration have a persistent and significant influence on long-term hydrological drought assessments.

Regarding the interaction effects, the GCM:SSP interaction was the most consistently significant, highlighting that the projected drought severity under a specific GCM is highly dependent on the emission scenario. Moreover, interactions involving calibration factors, particularly GCM:HC, GCM:PL, and HC:PL, were also found to be statistically significant

across all basins and decades. This indicates that the uncertainty from calibration conditions does not merely add to the total uncertainty but also modulates the uncertainty stemming from climate models, which is a critical consideration for developing robust drought management strategies. In contrast, other interactions such as SSP:HC and SSP:PL were found to be not significant across the basins and decades.

3.9.3 Uncertainty contribution of future hydrological drought

The quantification of uncertainty in future hydrological drought was conducted using ANOVA. The uncertainty in future hydrological drought projections caused by SSP, GCM, and hydrological modelling parameters was clearly quantified by ANOVA. Fig S.10 shows the contribution of each factor to the total uncertainty. Among single-factor uncertainties, GCM contributed the most, averaging over 30%. The largest contributor to the total uncertainty, however, was the interaction between SSP and GCM, averaging over 50%.

Fig. 7 and Table 8 present the contribution of hydrological modelling parameters to the uncertainty in future drought projections. The uncertainty contribution from hydrological model parameter estimation in future hydrological drought analysis averaged 2.7%, which is lower than that observed for future runoff projections. The uncertainty contribution from hydrological model calibration for future drought conditions was highest in HC, followed by CJ, AD, and SJ, respectively. These results differ from those obtained in the runoff projections. The contribution of uncertainty in hydrological drought analysis decreased for AD and SJ, where uncertainty in future runoff projection due to hydrological model calibration was relatively high. In contrast, HC showed high uncertainty contributions from hydrological model calibration in both runoff and drought analyses. Monthly runoff is a direct physical variable with high temporal volatility. In contrast, the SDI, used here to quantify hydrological drought, is a processed statistical indicator. It is calculated by accumulating and standardizing runoff over multi-month timescales. This integration process acts as a filter, effectively smoothing the high-frequency variability of the raw runoff series. Consequently, the absolute numerical fluctuation of the SDI is significantly smaller than that of the runoff itself. This reduced total variance in the drought index is the primary reason why the quantified uncertainty contributions appear lower and exhibit a different pattern compared to the runoff analysis. This highlights that while the underlying drivers of uncertainty are the same, their manifestation can differ depending on the temporal scale and the nature of the hydrological variable being

589 analyzed. These findings confirm the necessity to separately analyze and consider uncertainties
590 in future runoff projection and hydrological drought analysis.

591

592 **4. Discussion**

593 This study quantified the cascade of uncertainties caused by various factors in the process of
594 projecting future runoff and analyzing future hydrological drought. Previous studies
595 (Chegwidden et al., 2019; Wang et al., 2020) have reported that climate data from GCMs and
596 SSP scenarios are the primary sources of uncertainty in future hydrological analysis. The
597 results of this study also identified GCMs as the major contributor to uncertainty in future
598 hydrological analysis. However, recent research has begun to identify and quantify the cascade
599 of uncertainties caused by factors beyond GCMs and SSP scenarios (Chen et al., 2022; Shi et
600 al., 2022). This study focused on the uncertainties inherent in the calibration of hydrological
601 models, which are essential for future water resource management. Rather than seeking a single
602 optimal parameter set, the central aim of this study was to quantify the uncertainty that arises
603 from this very choice.

604 There have been limited studies that consider the uncertainties in runoff projection due to
605 various calibrated parameter cases (Lee et al., 2021a). However, this study further subdivided
606 the observation data used in the calibration period of hydrological model parameters by the
607 amount of data and hydrological conditions to quantify the uncertainties more precisely. The
608 results showed that hydrological conditions had a greater impact than the amount of calibration
609 data period on the uncertainties in the calibration of hydrological model parameters.

610 This study went beyond merely projecting future runoff by also quantifying the cascade of
611 uncertainties in the analysis of future hydrological drought using this runoff projection. Many
612 studies on future drought prediction reported that hydrological drought becomes more complex
613 and uncertain due to its association with human activities and the use of future climate data and
614 hydrological models (Ashrafi et al., 2020; Satoh et al., 2022). Most existing studies on future
615 hydrological drought analysis focused on the severity and frequency of droughts. However,
616 this study quantified the cascade of uncertainties that arise in the process of future drought
617 analysis. Although the contribution of hydrological model uncertainty to future hydrological
618 drought may be lower compared to future runoff projections, the characteristics of uncertainty
619 differ between drought and runoff projections, clearly indicating the necessity to separately
620 analyze and consider these uncertainties in future hydrological analyses.

5. Conclusion

This study aimed to quantify the uncertainties in future runoff projections and hydrological drought analysis, considering various climate change scenarios and hydrological model calibrations. The SWAT model was used, and hydrological conditions were classified using the SDI. Additionally, 20 GCMs and three SSP scenarios were applied. The calibration data length ranged from 1 to 20 years, considering different hydrological conditions (Dry, Normal, Wet).

The main findings are as follows:

First, the validation performance of the calibrated hydrological model parameters depended significantly on the hydrological conditions of the calibration data. The hydrological model parameters calibrated with dry period data showed 11.4% higher performance under dry conditions and 6.1% higher performance under normal conditions.

Second, the contribution of hydrological model uncertainty to future runoff projections ranged from 3.9% to 9.8%, with this uncertainty being more pronounced during low runoff periods. ANOVA results clearly indicated that GCMs contributed the most uncertainty, consistently accounting for over 60% on average, highlighting GCMs as the dominant source. In contrast, the contributions of SSP scenarios and hydrological model parameters were relatively smaller.

Third, the contribution of hydrological model uncertainty in future hydrological drought analysis was on average 2.7%, lower than that observed for future runoff projections. The uncertainty contributions varied by basin, showing different patterns from runoff projections, thus confirming the necessity for separate analyses of future runoff and hydrological drought uncertainties.

The significance of this study lies in emphasizing the quantification of uncertainty from various sources, including hydrological conditions and calibration data length, in addition to climate model scenarios. The systematic approach using ANOVA provided insights into the dominant sources and interactions of uncertainties, offering important guidance for improving hydrological modeling practices and water resources planning under future climate scenarios. However, there remains a need to apply this methodology to other regions to generalize these findings further.

651

Competing interests

The contact author has declared that none of the authors has any competing interests.

Acknowledgement

This study was supported by of National Research Foundation of Korea (2021R1A2C2005699).

657

References

Abdulai, P. J., Chung, E.S.: Uncertainty assessment in drought severities for the Cheongmicheon watershed using multiple GCMs and the reliability ensemble averaging method, Sustainability, 11(16), 4283, https://doi.org/10.3390/su11164283, 2019

Arsenault, R., Brissette, F., & Martel, J. L.: The hazards of split-sample validation in hydrological model calibration, J Hydrol, 566, 346-362, https://doi.org/10.1016/j.jhydrol.2018.09.027, 2018

Ashrafi, S. M., Gholami, H., & Najafi, M. R.: Uncertainties in runoff projection and hydrological drought assessment over Gharesu basin under CMIP5 RCP scenarios, J Water Clim Chang, 11(S1), 145-163, https://doi.org/10.2166/wcc.2020.088, 2020

Bai, P., Liu, X., & Xie, J.: Simulating runoff under changing climatic conditions: a comparison of the long short-term memory network with two conceptual hydrologic models, J Hydrol, 592, 125779, https://doi.org/10.1016/j.jhydrol.2020.125779, 2021

Bosshard, T., Carambia, M., Goergen, K., Kotlarski, S., Krahe, P., Zappa, M., & Schär, C.: Quantifying uncertainty sources in an ensemble of hydrological climate-impact projections, Water Resour Res, 49(3), 1523-1536, https://doi.org/10.1029/2011WR011533, 2013

Broderick, C., Matthews, T., Wilby, R. L., Bastola, S., & Murphy, C.: Transferability of hydrological models and ensemble averaging methods between contrasting climatic periods, Water Resour Res, 52(10), 8343-8373, https://doi.org/10.1002/2016WR018850, 2016

679   Chae, S. T., Chung, E. S., & Jiang, J.: Enhancing Water Cycle Restoration through LID

680   Practices Considering Climate Change: A Study on Permeable Pavement Planning by an

681   Iterative MCDM Model, Water Resour Manag, 38(9), 3413-3428,

682   https://doi.org/10.1007/s11269-024-03821-z, 2024

683   Chae, S.T. Chung, E.S., Kim, D.: Evaluation of optimized multi-model ensembles for

684   extreme precipitation projection considering various objective functions, Water Resour, 1-19,

685   https://doi.org/10.1007/s11269-024-03948-z, 2024

686   Chegwidden, O. S., Nijssen, B., Rupp, D. E., Arnold, J. R., Clark, M. P., Hamman, J. J., Kao,

687   S.-C., Mao, Y., Mizukami, N., Mote, P.W., Pan, M., Pytlak, E., & Xiao, M.: How do

688   modeling decisions affect the spread among hydrologic climate change projections?

689   Exploring a large ensemble of simulations across a diversity of hydroclimates, Earths

690   Future, 7(6), 623-637, https://doi.org/10.1029/2018EF001047, 2019

691   Chen, C., Gan, R., Feng, D., Yang, F., & Zuo, Q.: Quantifying the contribution of SWAT

692   modeling and CMIP6 inputting to streamflow prediction uncertainty under climate change, J

693   Clean Prod, 364, 132675, https://doi.org/10.1016/j.jclepro.2022.132675, 2022

694   Coron, L., Andréassian, V., Perrin, C., Lerat, J., Vaze, J., Bourqui, M., & Hendrickx, F.:

695   Crash testing hydrological models in contrasted climate conditions: An experiment on 216

696   Australian catchments, Water Resour Res, 48(5), https://doi.org/10.1029/2011WR011721,

697   2012

698   Dakhlaoui, H., Ruelland, D., Tramblay, Y., & Bargaoui, Z.: Evaluating the robustness of

699   conceptual rainfall-runoff models under climate variability in northern Tunisia, J

700   Hydrol, 550, 201-217, https://doi.org/10.1016/j.jhydrol.2017.04.032, 2017

701   Devia, G. K., Ganasri, B. P., & Dwarakish, G. S.: A review on hydrological

702   models, Aquat Procedia. 4, 1001-1007, https://doi.org/10.1016/j.aqpro.2015.02.126, 2015

703   Feng, K., Zhou, J., Liu, Y., Lu, C., & He, Z.: Hydrological uncertainty processor (HUP) with

704   estimation of the marginal distribution by a Gaussian mixture model, Water Resour

705   Manag, 33, 2975-2990, https://doi.org/10.1007/s11269-019-02260-5, 2019

706   Fowler, K. J., Peel, M. C., Western, A. W., Zhang, L., & Peterson, T. J.: Simulating runoff

707   under changing climatic conditions: Revisiting an apparent deficiency of conceptual rainfall-

708   runoff models, Water Resour Res. 52(3), 1820-1846,

709   https://doi.org/10.1002/2015WR018068, 2016

710   Ghasemizade, M., & Schirmer, M.: Subsurface flow contribution in the hydrological cycle:

711   lessons learned and challenges ahead—a review, Environ Earth Sci. 69, 707-718,

712   https://doi.org/10.1007/s12665-013-2329-8, 2013

713   Gudmundsson, L., Bremnes, J. B., Haugen, J. E., & Engen-Skaugen, T.: Downscaling RCM

714   precipitation to the station scale using statistical transformations–a comparison of

715   methods, Hydrol Earth Syst Sci, 16(9), 3383-3390, https://doi.org/10.5194/hess-16-3383-

716   2012, 2012

717   Gupta, H. V., Kling, H., Yilmaz, K. K., & Martinez, G. F.: Decomposition of the mean

718   squared error and NSE performance criteria: Implications for improving hydrological

719   modelling, J Hydrol, 377(1-2), 80-91, https://doi.org/10.1016/j.jhydrol.2009.08.003, 2009

720   Hanel, M., & Buishand, T. A.: Assessment of the sources of variation in changes of

721   precipitation characteristics over the Rhine basin using a linear mixed-effects model. J

722   Clim., 28(17), 6903-6919, https://doi.org/10.1175/JCLI-D-14-00775.1, 2015

723   Hong, X., Guo, S., Zhou, Y., & Xiong, L.: Uncertainties in assessing hydrological drought

724   using streamflow drought index for the upper Yangtze River basin, Stoch Environ

725   Res Risk Assess, 29, 1235-1247, https://doi.org/10.1007/s00477-014-0949-5, 2015

726   IPCC: IPCC Climate Change 2014: Synthesis Report. Contribution of Working Groups I, II

727   and III to the Fifth Assessment Report of the Intergovernmental Panel on Climate Change,

728   IPCC, Geneva, Switzerland, 2014

729   IPCC.: Summary for Policymakers. In: Climate Change 2021: The Physical Science Basis.

730   Contribution of Working Group I to the Sixth Assessment Report of the Intergovernmental

731   Panel on Climate Change [Masson-Delmotte, V., P. Zhai, A. Pirani, S. L. Connors, C. Péan,

732   S. Berger, N. Caud, Y. Chen, L. Goldfarb, M. I. Gomis, M. Huang, K. Leitzell, E. Lonnoy,

733   J.B.R. Matthews, T. K. Maycock, T. Waterfield, O. Yelekçi, R. Yu and B. Zhou (eds.)].

734   Cambridge University Press. In Press, 2021

735   Karunakalage, A., Lee, J. Y., Daqiq, M. T., Cha, J., Jang, J., & Kannaujiya, S.:

736   Characterization of groundwater drought and understanding of climatic impact on

737   groundwater resources in Korea, J Hydrol, 634, 131014,

738   https://doi.org/10.1016/j.jhydrol.2024.131014, 2024

739   Kim, H. S., Croke, B. F., Jakeman, A. J., & Chiew, F. H.: An assessment of modelling

740   capacity to identify the impacts of climate variability on catchment hydrology, Math Comput

741   Simul. 81(7), 1419-1429, https://doi.org/10.1016/j.matcom.2010.05.007, 2011

742   Kim, J. H., Sung, J. H., Chung, E. S., Kim, S. U., Son, M., & Shiru, M. S.: Comparison of

743   Projection in Meteorological and Hydrological Droughts in the Cheongmicheon Watershed

744   for RCP4. 5 and SSP2-4.5, Sustainability, 13(4), 2066, https://doi.org/10.3390/su13042066,

745   2021

746   Kim, J. H., Sung, J. H., Shahid, S., & Chung, E. S.: Future hydrological drought analysis

747   considering agricultural water withdrawal under SSP scenarios, Water Resour Manag, 36(9),

748   2913-2930, https://doi.org/10.1007/s11269-022-03116-1, 2022

749   Lee, S., Qi, J., McCarty, G. W., Yeo, I. Y., Zhang, X., Moglen, G. E., & Du, L.: Uncertainty

750   assessment of multi-parameter, multi-GCM, and multi-RCP simulations for streamflow and

751   non-floodplain wetland (NFW) water storage, J Hydrol, 600, 126564,

752   https://doi.org/10.1016/j.jhydrol.2021.126564, 2021

753   Lee, S., Lee, S. J., Jang, K., & Chun, J. H.: Drought monitoring based on vegetation type and

754   reanalysis data in Korea, Atmosphere, 12(2), 170,

755   https://doi.org/10.1016/j.jhydrol.2021.126564, 2021

756   Mahabadi, S. A., & Delavar, M.: Evaluation and comparison of different methods for

757   determining the contribution of climatic factors and direct human interventions in reducing

758   basin discharge, Ecol Indic, 158, 111480, https://doi.org/10.1016/j.ecolind.2023.111480,

759   2024

760   Merz, R., Parajka, J., & Blöschl, G.: Time stability of catchment model parameters:

761   Implications for climate impact analyses, Water Resour Res, 47(2),

762   https://doi.org/10.1029/2010WR009505, 2011

763   Milly, P. C., Betancourt, J., Falkenmark, M., Hirsch, R. M., Kundzewicz, Z. W., Lettenmaier,

764   D. P., & Stouffer, R. J., 2008. Stationarity is dead: Whither water

765   management?. Science. 319(5863), 573-574.

766 Mo, C., Huang, K., Ruan, Y., Lai, S., & Lei, X.: Quantifying uncertainty sources in runoff
767 change attribution based on the Budyko framework, J Hydrol, 630, 130790,
768 https://doi.org/10.1016/j.jhydrol.2024.130790, 2024

769 Morim, J., M. Hemer, X.L. Wang, N. Cartwright, C. Trenham, A. Semedo, I. Young, L.
770 Bricheno, P. Camus, M. Casas-Prat, L.i. Erikson, L. Mentaschi, N. Mori, T. Shimura, B.
771 Timmermans, O. Aarnes, Ø. Breivik, A. Behrens, M. Dobrynin, M. Menendez, J. Staneva, M.
772 Wehner, J. Wolf, B. Kamranzad, A. Webb, J. Stopa, F. Andutta.: Robustness and
773 uncertainties in global multivariate wind-wave climate projections, Nat Clim Chang, 9(9),
774 711-718, https://doi.org/10.1038/s41558-019-0542-5, 2019

775 Nalbantis, I., & Tsakiris, G.: Assessment of hydrological drought revisited, Water Resour
776 Manag, 23, 881-897, https://doi.org/10.1007/s11269-008-9305-1, 2009

777 Nguyen, T. V., Dietrich, J., Dang, T. D., Tran, D. A., Van Doan, B., Sarrazin, F. J.,
778 Abbaspour, K., & Srinivasan, R.: An interactive graphical interface tool for parameter
779 calibration, sensitivity analysis, uncertainty analysis, and visualization for the Soil and Water
780 Assessment Tool, Environ Model Softw, 156, 105497,
781 https://doi.org/10.1016/j.envsoft.2022.105497, 2022

782 O'Neill, B. C., Tebaldi, C., Van Vuuren, D. P., Eyring, V., Friedlingstein, P., Hurtt, G.,
783 Knutti, R., Kriegler, E., Lamarque, J.F., Lowe, J., Meehl, J., Moss, R., Riahi, K., Sanderson,
784 B. M.: The scenario model intercomparison project (ScenarioMIP) for
785 CMIP6, Geosci Model Dev, 9(9), 3461-3482, https://doi.org/10.5194/gmd-9-3461-2016,
786 2016

787 Peng, A., Zhang, X., Xu, W., & Tian, Y.: Effects of training data on the learning performance
788 of LSTM network for runoff simulation, Water Resour Manag t, 36(7), 2381-2394,
789 https://doi.org/10.1007/s11269-022-03148-7, 2022

790 Perrin, C., Oudin, L., Andreassian, V., Rojas-Serna, C., Michel, C., & Mathevet, T.: Impact
791 of limited streamflow data on the efficiency and the parameters of rainfall—runoff
792 models, Hydrol Sci J, 52(1), 131-151, https://doi.org/10.1623/hysj.52.1.131, 2007

793 Qi, W., Zhang, C., Fu, G., Sweetapple, C., & Zhou, H.: Evaluation of global fine-resolution
794 precipitation products and their uncertainty quantification in ensemble discharge
795 simulations, Hydrol Earth Syst Sci, 20(2), 903-920, https://doi.org/10.5194/hess-20-903-
796 2016, 2016

797 Razavi, S., & Tolson, B. A.: An efficient framework for hydrologic model calibration on long
798 data periods, Water Resour Res, 49(12), 8418-8431, https://doi.org/10.1002/2012WR013442,
799 2013

800 Renard, B., Kavetski, D., Kuczera, G., Thyer, M., & Franks, S. W.: Understanding predictive
801 uncertainty in hydrologic modeling: The challenge of identifying input and structural
802 errors, Water Resour Res, 46(5), https://doi.org/10.1029/2009WR008328, 2010

803 Saft, M., Peel, M. C., Western, A. W., Perraud, J. M., & Zhang, L.: Bias in streamflow
804 projections due to climate-induced shifts in catchment response, Geophys Res Lett, 43(4),
805 1574-1581, https://doi.org/10.1002/2015GL067326, 2016

806 Santos, C. A. G., Neto, R. M. B., do Nascimento, T. V. M., da Silva, R. M., Mishra, M., &
807 Frade, T. G.: Geospatial drought severity analysis based on PERSIANN-CDR-estimated
808 rainfall data for Odisha state in India (1983–2018), Sci Total Environ, 750, 141258,
809 https://doi.org/10.1016/j.scitotenv.2020.141258, 2021

810 Satoh, Y., Yoshimura, K., Pokhrel, Y., Kim, H., Shiogama, H., Yokohata, T., Hanasaki, N.,
811 Wada, Y., Burek, P., Byers, E., Schmied, H. M., Gerten, D., Ostberg, S., Gosling, S. N.,
812 Boulange, J. E. S., & Oki, T.: The timing of unprecedented hydrological drought under
813 climate change, Nat Commun, 13(1), 3287, https://doi.org/10.1038/s41467-022-30729-2,
814 2022

815 Sheffield, J., & Wood, E. F.: Drought: past problems and future scenarios. Routledge,
816 https://doi.org/10.4324/9781849775250, 2012

817 Shi, L., Feng, P., Wang, B., Li Liu, D., Zhang, H., Liu, J., & Yu, Q.: Assessing future runoff
818 changes with different potential evapotranspiration inputs based on multi-model ensemble of
819 CMIP5 projections, J Hydrol, 612, 128042, https://doi.org/10.1016/j.jhydrol.2022.128042,
820 2022

821 Song, Y. H., Chung, E. S., & Shahid, S.: Differences in extremes and uncertainties in future
822 runoff simulations using SWAT and LSTM for SSP scenarios, Sci Total Environ, 838,
823 156162, https://doi.org/10.1016/j.scitotenv.2022.156162, 2022

824 Sun, W., Wang, Y., Wang, G., Cui, X., Yu, J., Zuo, D., & Xu, Z.: Physically based
825 distributed hydrological model calibration based on a short period of streamflow data: case

826   studies in four Chinese basins, Hydrol Earth Syst Sci, 21(1), 251-265,

827   https://doi.org/10.5194/hess-21-251-2017, 2017

828   Sung, J. H., Chung, E. S., & Shahid, S.: Reliability–Resiliency–Vulnerability approach for

829   drought analysis in South Korea using 28 GCMs, Sustainability, 10(9), 3043,

830   https://doi.org/10.3390/su10093043, 2018

831   Thirel, G., Andréassian, V., & Perrin, C.: On the need to test hydrological models under

832   changing conditions, Hydrol Sci J, 60(7-8), 1165-1173,

833   https://doi.org/10.1080/02626667.2015.1050027, 2015

834   Vetter, T., Huang, S., Aich, V., Yang, T., Wang, X., Krysanova, V., & Hattermann, F.: Multi-

835   model climate impact assessment and intercomparison for three large-scale river basins on

836   three continents, Earth Syst Dyn, 6(1), 17-43, https://doi.org/10.5194/esd-6-17-2015, 2015

837   Wang, H. M., Chen, J., Xu, C. Y., Zhang, J., & Chen, H.: A framework to quantify the

838   uncertainty contribution of GCMs over multiple sources in hydrological impacts of climate

839   change, Earths Future, 8(8), e2020EF001602, https://doi.org/10.1029/2020EF001602, 2020

840   Xu, Z., Godrej, A. N., & Grizzard, T. J.: The hydrological calibration and validation of a

841   complexly-linked watershed–reservoir model for the Occoquan watershed, Virginia, J

842   Hydrol, 345(3-4), 167-183, https://doi.org/10.1016/j.jhydrol.2007.07.015, 2007

843   Yang, G., Giuliani, M., & Galelli, S.: Valuing the codesign of streamflow forecast and

844   reservoir operation models, J Water Resour Plan Manag, 149(8), 04023037,

845   https://doi.org/10.1061/JWRMD5.WRENG-6023, 2023

846   Yang, X., Chen, Z., & Qin, M.: Monthly Runoff Prediction Via Mode Decomposition-

847   Recombination Technique, Water Resour Manag, 38(1), 269-286,

848   https://doi.org/10.1007/s11269-023-03668-w, 2023

849   Yip, S., Ferro, C. A., Stephenson, D. B., & Hawkins, E.: A simple, coherent framework for

850   partitioning uncertainty in climate predictions, J Clim Change, 24(17), 4634-4643,

851   https://doi.org/10.1175/2011JCLI4085.1, 2011

852   Yu, Q., Jiang, L., Wang, Y., & Liu, J., 2023. Enhancing streamflow simulation using

853   hybridized machine learning models in a semi-arid basin of the Chinese loess Plateau. J

854   Hydrol. 617, 129115.

855   Yuan, Q., Thorarinsdottir, T. L., Beldring, S., Wong, W. K., & Xu, C. Y.: Assessing

856   uncertainty in hydrological projections arising from local-scale internal variability of

857   climate, J Hydrol, 620, 129415, https://doi.org/10.1016/j.jhydrol.2023.129115, 2023

858   Zhang, X., Song, S., & Guo, T.: Nonlinear Segmental Runoff Ensemble Prediction Model

859   Using BMA, Water Resour Manag, 1-18, https://doi.org/10.1007/s11269-024-03824-w, 2024

860   Ziarh, G. F., Kim, J. H., Song, J. Y., & Chung, E. S.: Quantifying Uncertainty in Runoff

861   Simulation According to Multiple Evaluation Metrics and Varying Calibration Data

862   Length, Water, 16(4), 517, https://doi.org/10.3390/w16040517, 2024

863

864
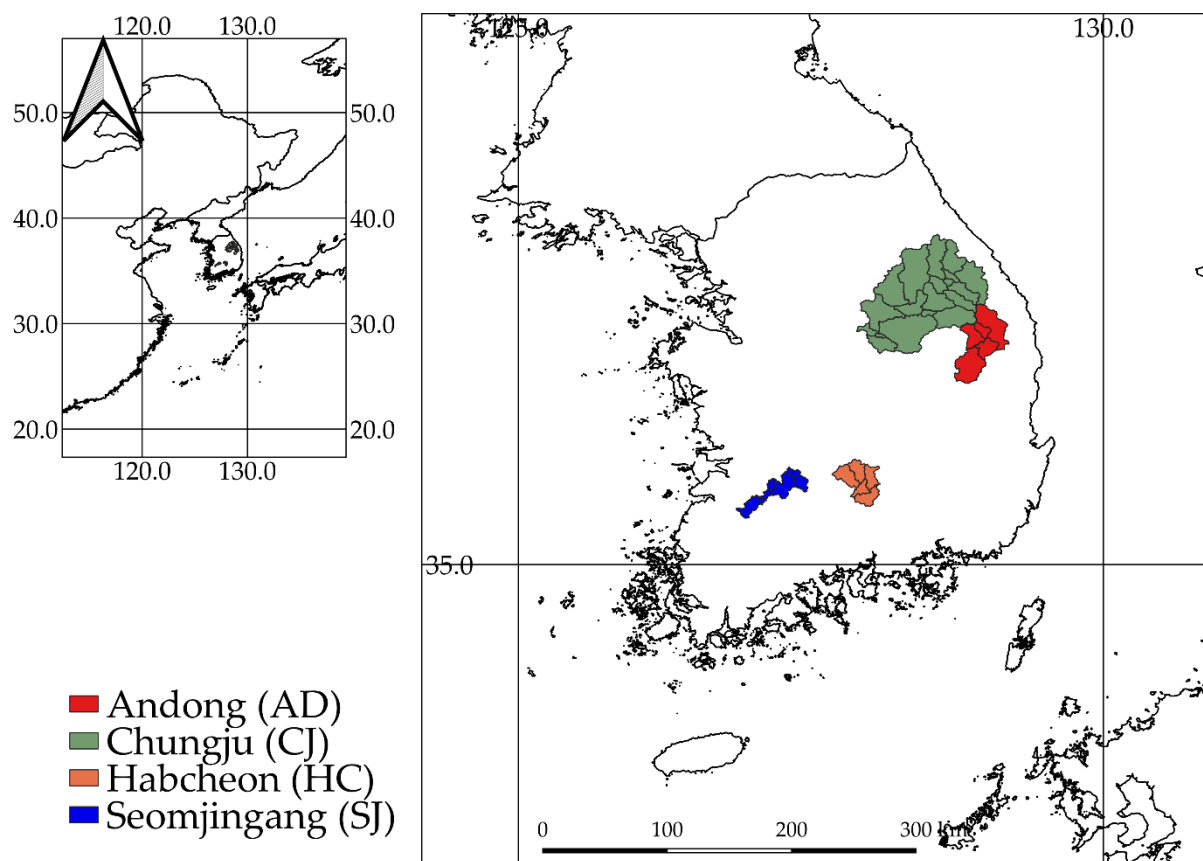
865

866 *Figure. 1. Description of study area.*

867

(a) AD

(b) CJ

(c) HC

(d) SJ

	25%~75%
	Min~Max
	Median Line
	Mean
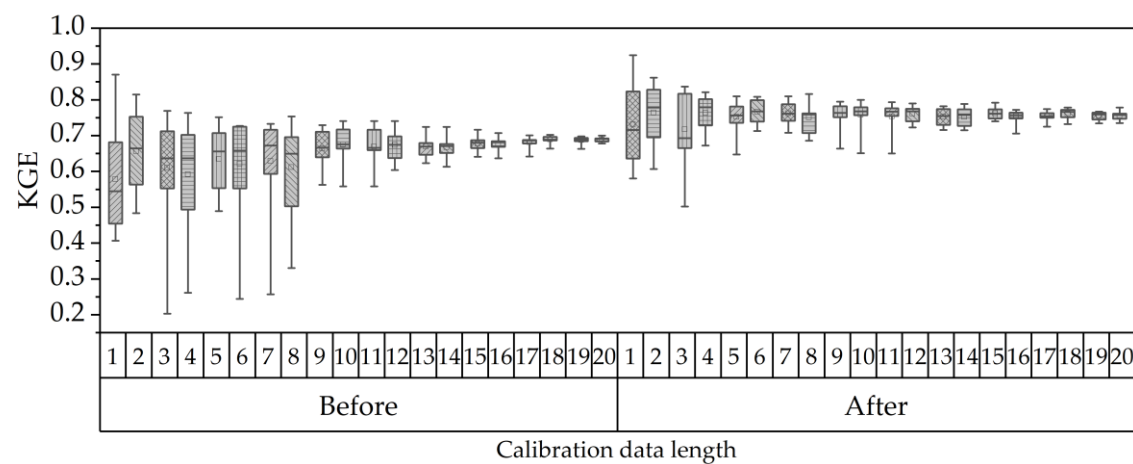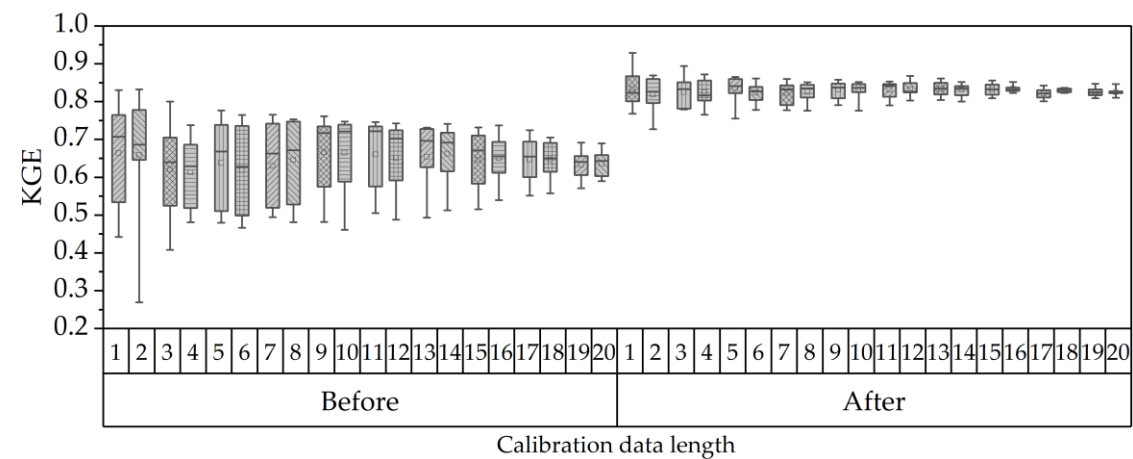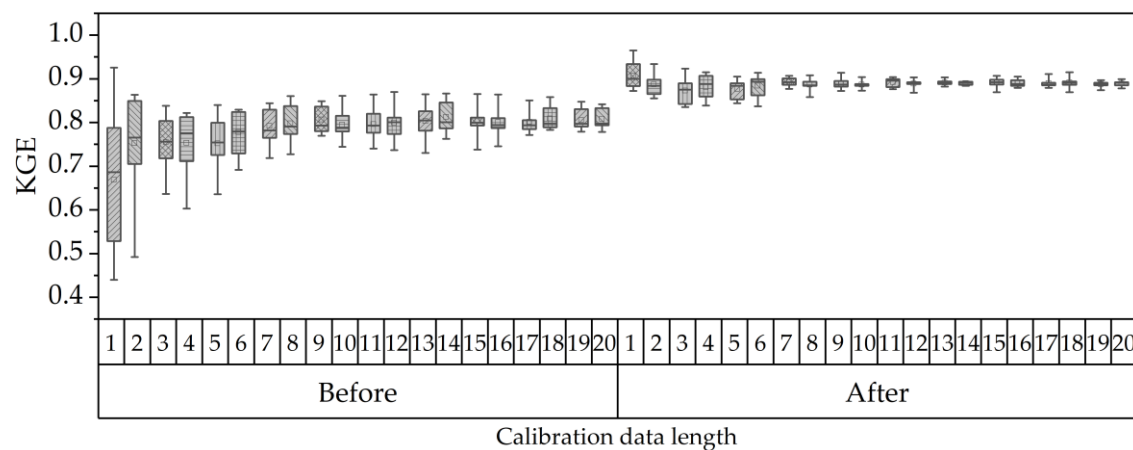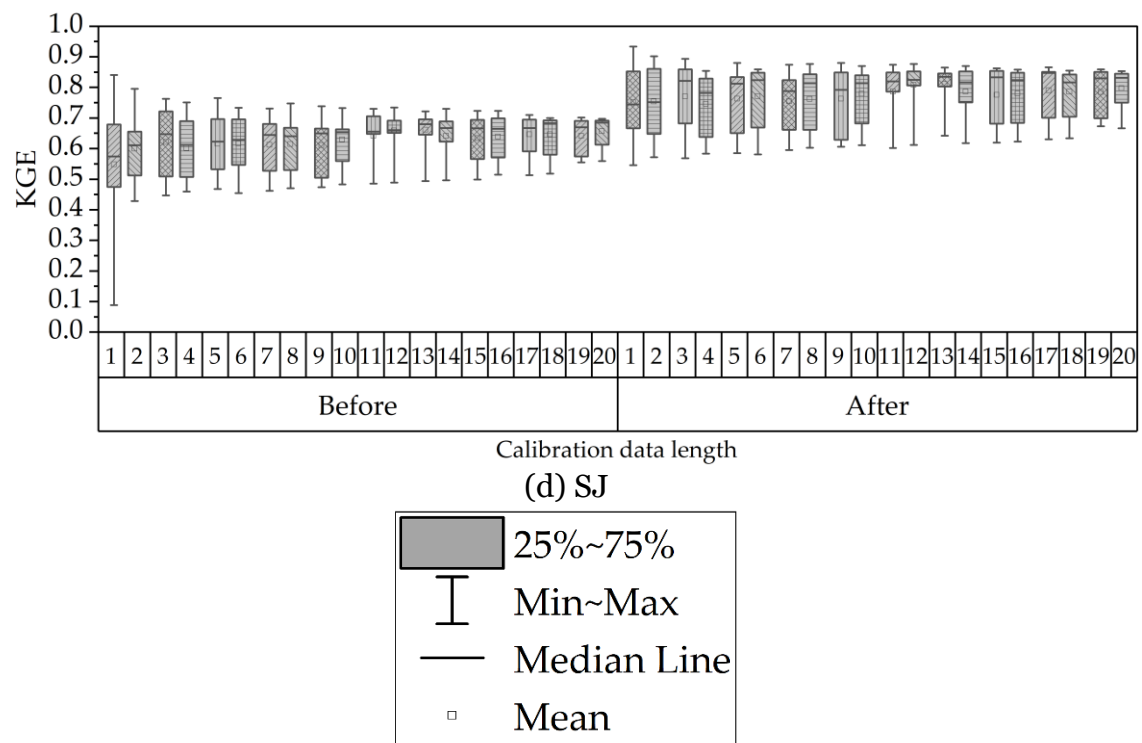
869   *Figure. 2. KGE values before and after calibration*

870

871
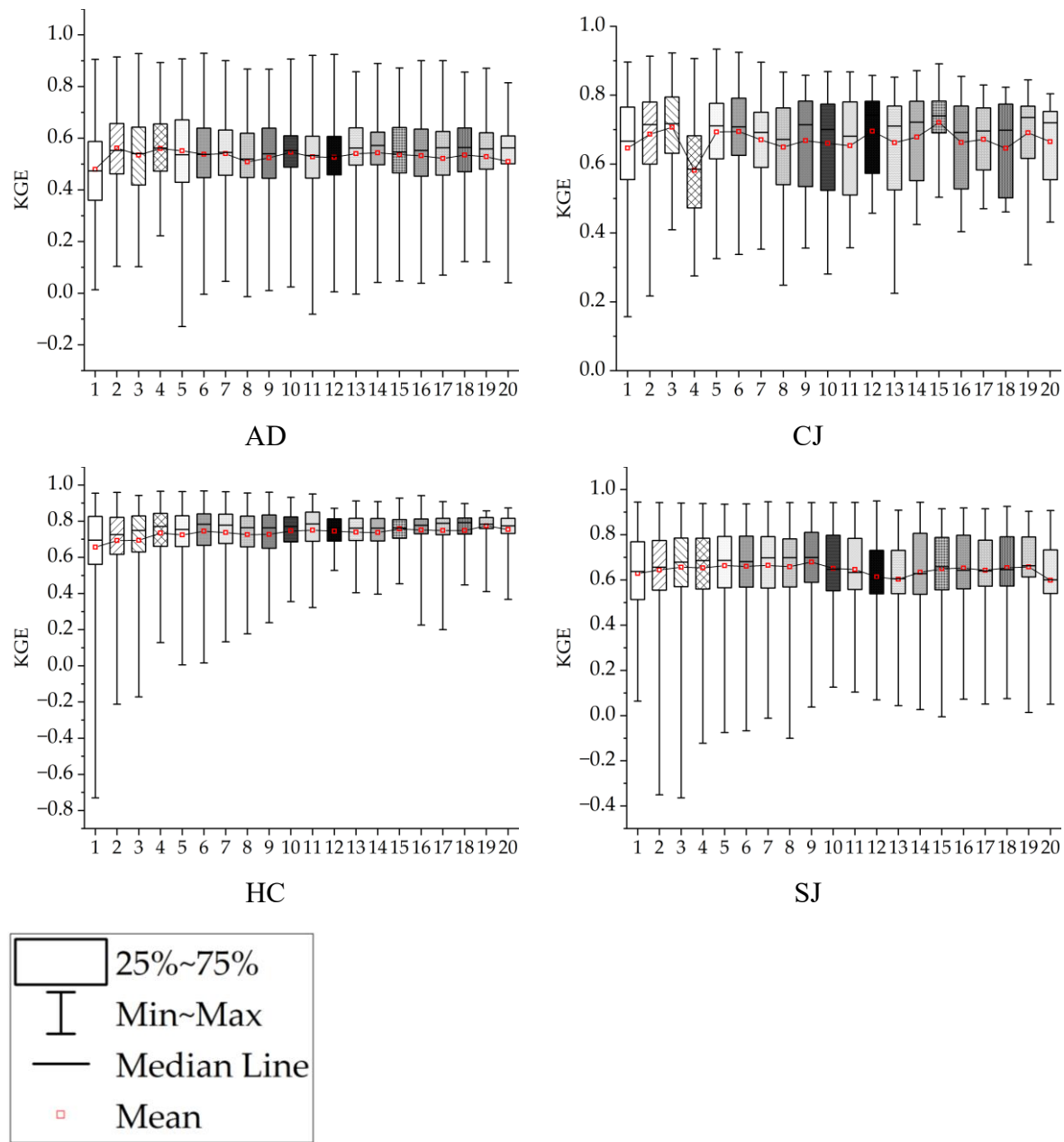
872   *Figure. 3. Validation performances depending on data length of the calibration period*

873

Basins   Hydrological conditions for validation period
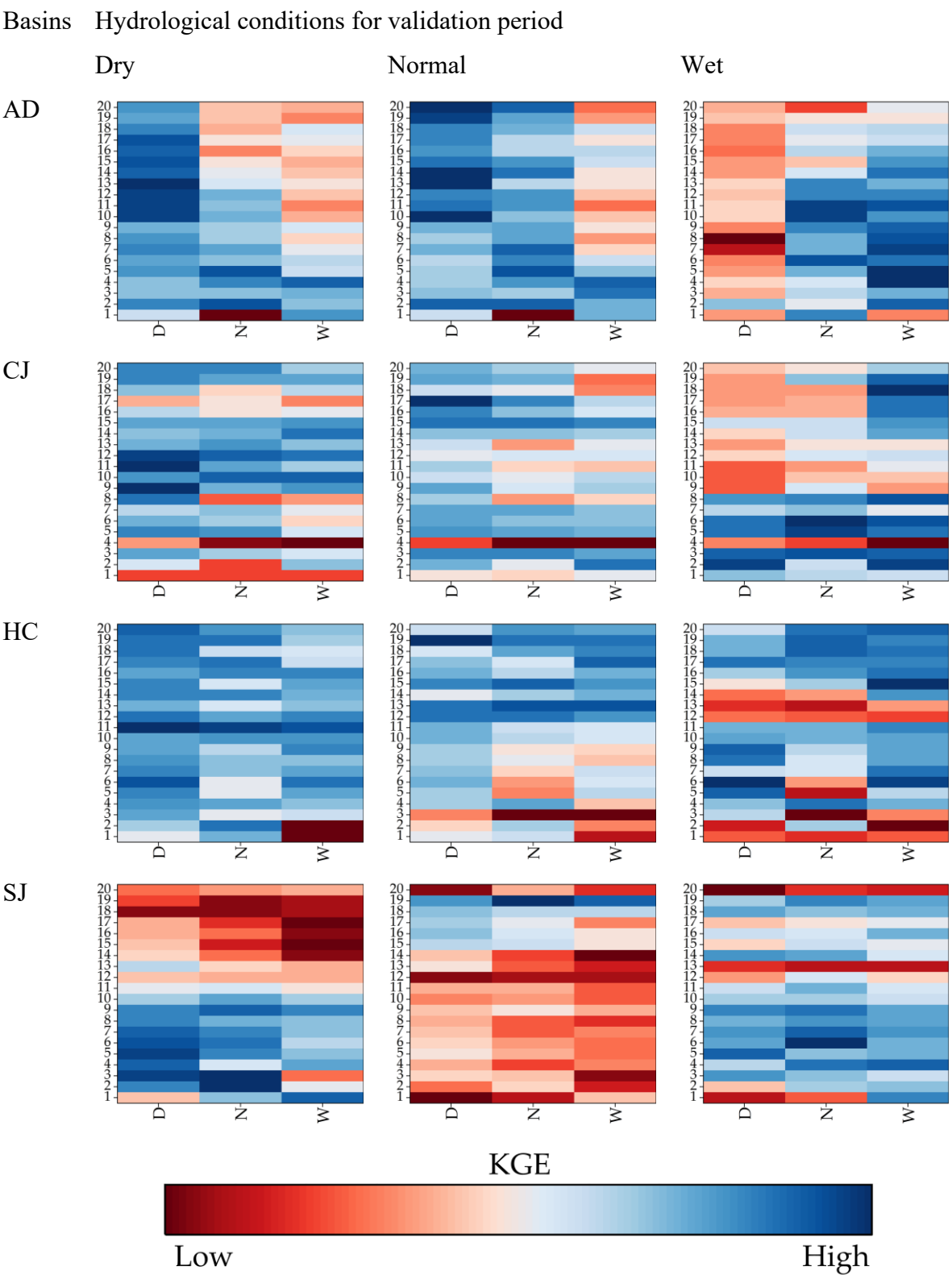
Figure. 4. KGEs classified by hydrological conditions for the calibration-validation period
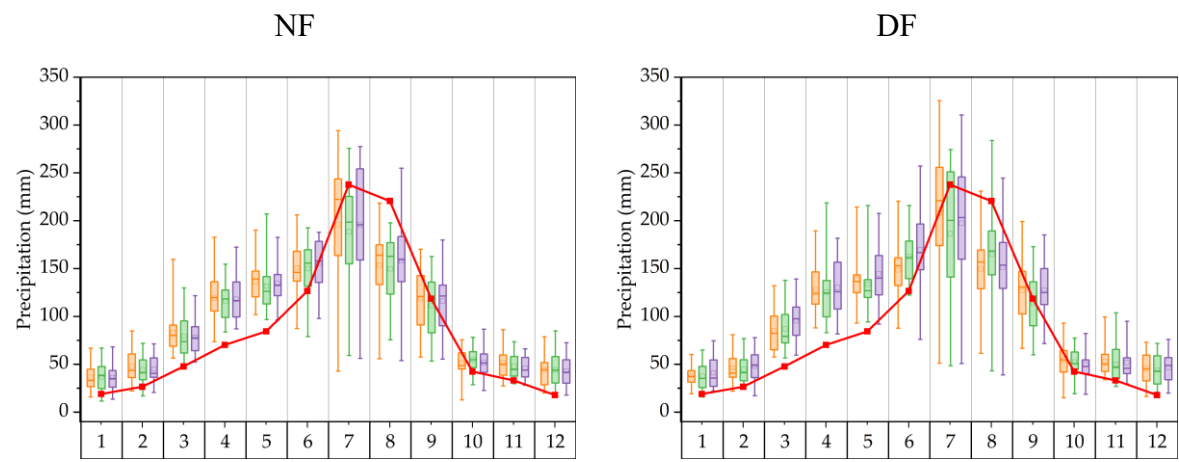
(a) Precipitation
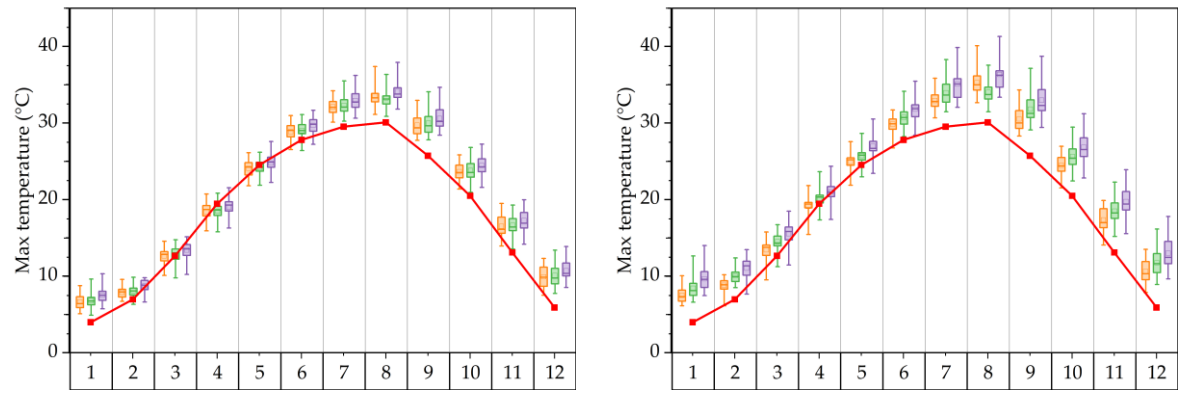
(b) Max temperature
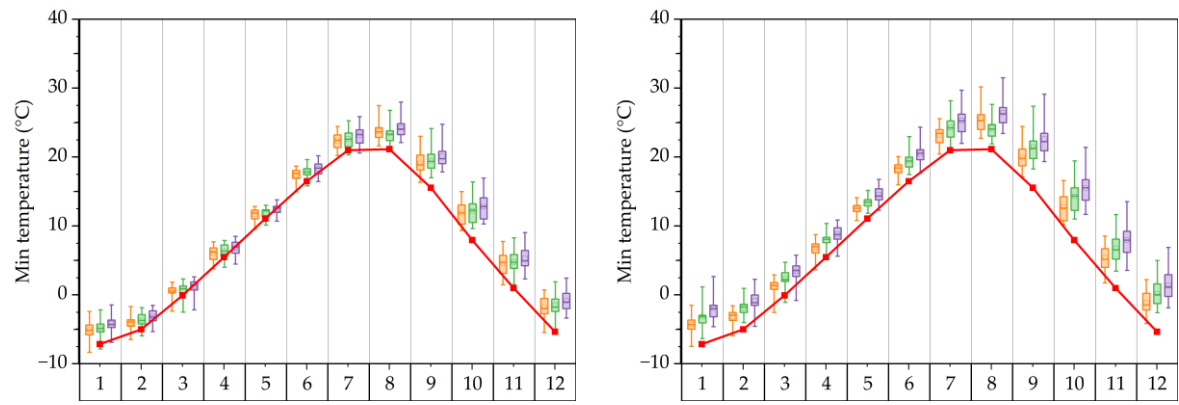
(c) Min temperature
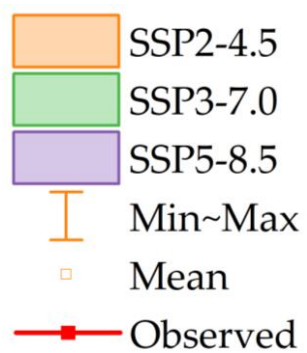
878

879   *Figure. 5. Projected annual changes in future precipitation (mm) and temperature (°C)*

880
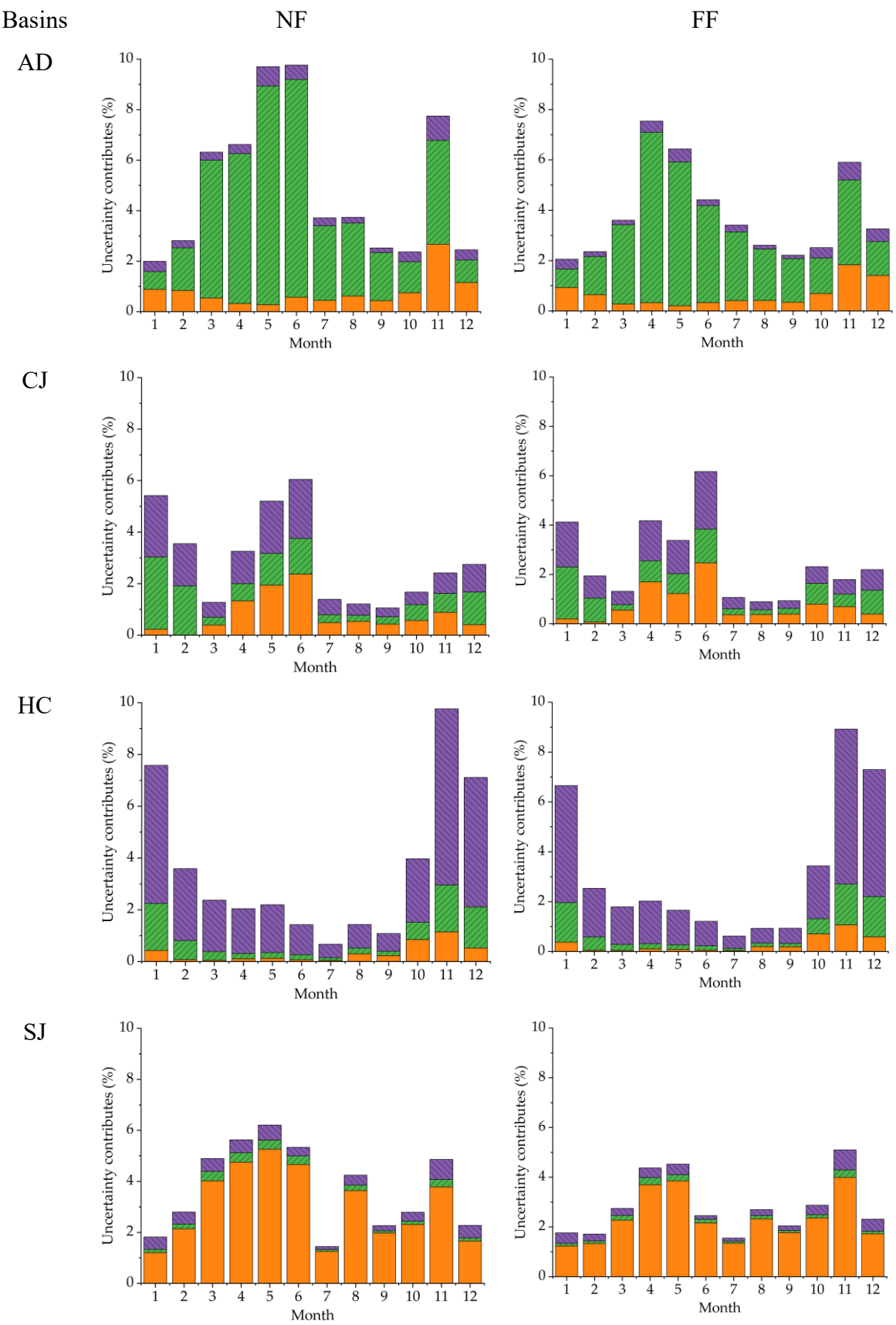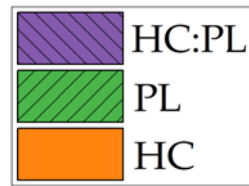
882 *Figure. 6. Contribution of hydrological model parameter to uncertainty in future runoff*

883 *projection using ANOVA*

884

885

(a) AD (b) CJ

(c) HC (d) SJ

886
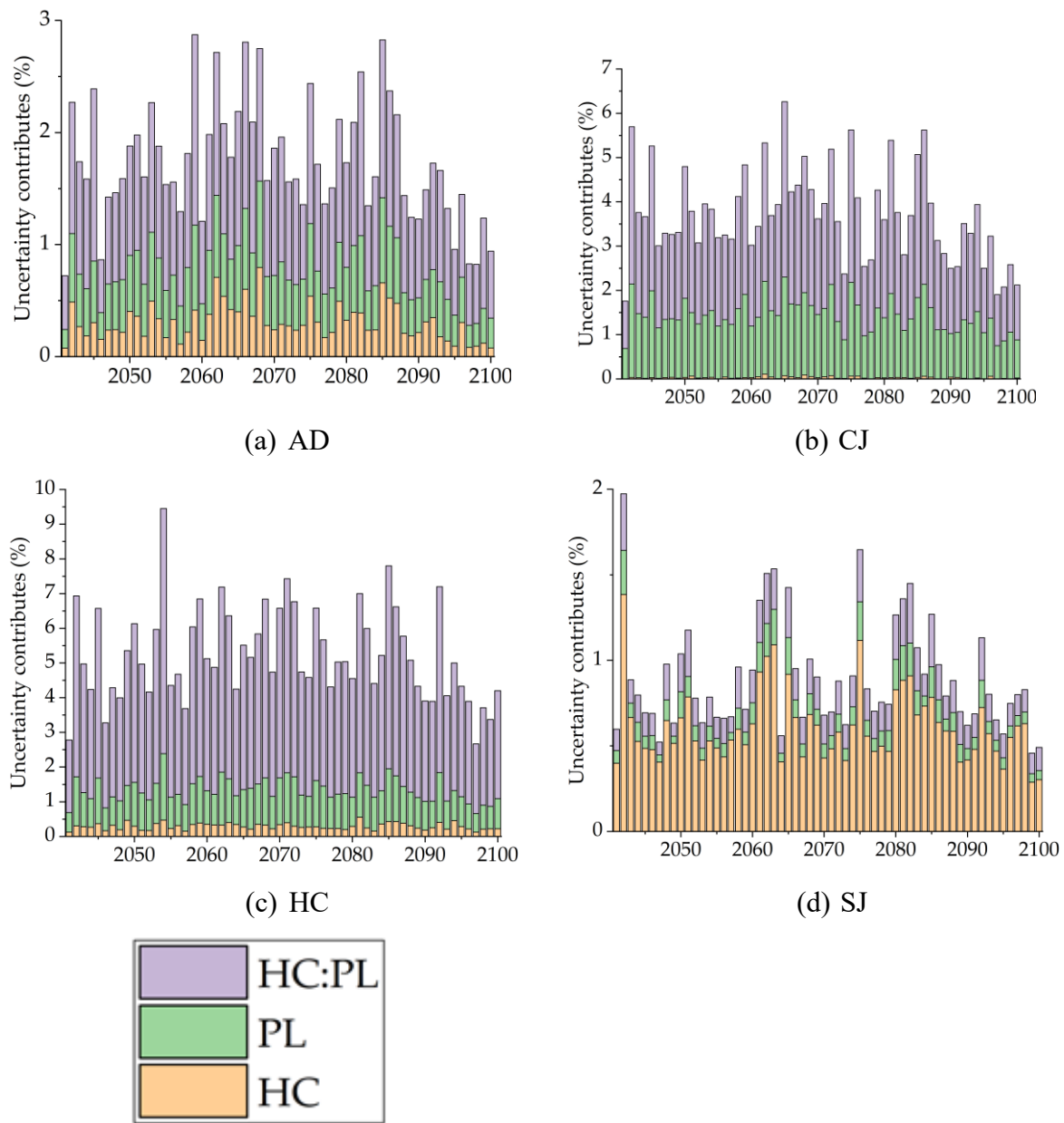
887 *Figure. 7. Contribution of hydrological model parameter to uncertainty in future*

888 *hydrological drought analysis*

889

890

891 *Table 1. Validation performance according to hydrological conditions*

Basins	Validation climatic conditions	Calibration period hydrological conditions		
		D	N	W
AD	D	0.480	0.401	0.382
	N	0.573	0.562	0.510
	W	0.571	0.621	0.642
CJ	D	0.743	0.727	0.725
	N	0.643	0.621	0.615
	W	0.674	0.686	0.706
HC	D	0.732	0.691	0.670
	N	0.738	0.719	0.714
	W	0.763	0.757	0.769
SJ	D	0.557	0.544	0.515
	N	0.677	0.671	0.650
	W	0.674	0.681	0.684

892

893

894   *Table 2. Changes from historical to future runoff for four dam basins*

895   (unit: %)

Basins	SSPs	NF				DF			
		Spring	Summer	Fall	Winter	Spring	Summer	Fall	Winter
AD	SSP2-4.5	82.1	-9.9	10.8	178.3	92.6	-5.3	18.1	179.2
	SS3-7.0	84.3	-11.1	6.7	168.3	104.3	-6.3	16.4	188.9
	SSP5-8.5	91.0	-5.7	12.9	194.2	118.9	1.2	26.7	216.1
CJ	SSP2-4.5	184.6	25.1	34.7	242.8	191.7	32.4	47.3	252.7
	SS3-7.0	186.6	21.0	32.8	226.7	210.2	27.6	44.7	276.5
	SSP5-8.5	148.8	8.0	0.8	173.1	157.2	14.0	13.1	192.0
HC	SSP2-4.5	207.6	2.7	-19.7	95.4	222.7	8.1	-12.3	100.8
	SS3-7.0	213.7	-1.3	-22.5	91.2	243.4	6.8	-12.7	109.0
	SSP5-8.5	223.2	5.7	-15.2	110.0	268.8	14.8	-3.3	127.4
SJ	SSP2-4.5	170.9	1.5	7.7	60.5	181.4	5.9	18.4	63.3
	SS3-7.0	175.1	-2.1	7.3	58.6	198.9	5.6	17.9	75.6
	SSP5-8.5	181.1	5.5	12.9	75.1	217.2	14.0	29.7	88.6

896

897

Table 3. Differences in low runoff according to hydrological model parameters

(unit: m³/s)

Basins	SSPs	NF		DF	
		Q_{75} Differ	Ratio (%)	Q_{75} Differ	Ratio (%)
AD	SSP2-4.5	7.24	10.28	7.00	10.42
	SSP3-7.0	7.04	9.58	7.71	9.56
	SSP5-8.5	7.43	9.32	7.88	9.94
CJ	SSP2-4.5	48.93	5.60	49.00	5.35
	SSP3-7.0	48.80	4.60	52.35	5.53
	SSP5-8.5	39.02	5.70	38.09	6.11
HC	SSP2-4.5	5.84	12.67	5.86	13.93
	SSP3-7.0	5.55	13.86	5.95	12.86
	SSP5-8.5	6.03	12.86	6.44	14.62
SJ	SSP2-4.5	4.61	9.84	4.51	9.61
	SSP3-7.0	4.23	11.24	4.64	9.76
	SSP5-8.5	4.64	9.37	4.97	9.12

902 *Table 4. Frequency of statistical significance (p < 0.05) of uncertainty sources for future*
903 *monthly runoff during the NF period*

Factor	Jan	Feb	Mar	Apr	May	Jun	Jul	Aug	Sep	Oct	Nov	Dec
GCM	4/4	4/4	4/4	4/4	4/4	4/4	4/4	4/4	4/4	4/4	4/4	4/4
SSP	4/4	4/4	4/4	4/4	4/4	4/4	4/4	4/4	4/4	4/4	4/4	4/4
HC	4/4	4/4	4/4	4/4	4/4	4/4	4/4	4/4	4/4	4/4	4/4	4/4
PL	4/4	4/4	4/4	4/4	4/4	4/4	4/4	4/4	4/4	4/4	4/4	4/4
GCM:SSP	4/4	4/4	4/4	4/4	4/4	4/4	4/4	4/4	4/4	4/4	4/4	4/4
GCM:HC	3/4	2/4	2/4	2/4	2/4	4/4	4/4	4/4	4/4	4/4	4/4	4/4
GCM:PL	4/4	4/4	4/4	4/4	4/4	4/4	4/4	4/4	4/4	4/4	4/4	4/4
SSP:HC	0/4	0/4	0/4	0/4	0/4	0/4	0/4	0/4	0/4	1/4	1/4	0/4
SSP:PL	0/4	0/4	0/4	0/4	0/4	1/4	2/4	1/4	0/4	1/4	0/4	0/4
HC:PL	4/4	4/4	4/4	4/4	4/4	4/4	4/4	4/4	4/4	4/4	4/4	4/4

904

Table 5. Frequency of statistical significance (p < 0.05) of uncertainty sources for future

monthly runoff during the DF period

Factor	Jan	Feb	Mar	Apr	May	Jun	Jul	Aug	Sep	Oct	Nov	Dec
GCM	4/4	4/4	4/4	4/4	4/4	4/4	4/4	4/4	4/4	4/4	4/4	4/4
SSP	4/4	4/4	4/4	4/4	4/4	4/4	4/4	4/4	4/4	4/4	4/4	4/4
HC	4/4	4/4	4/4	4/4	4/4	4/4	4/4	4/4	4/4	4/4	4/4	4/4
PL	4/4	4/4	4/4	4/4	4/4	4/4	4/4	4/4	4/4	4/4	4/4	4/4
GCM:SSP	4/4	4/4	4/4	4/4	4/4	4/4	4/4	4/4	4/4	4/4	4/4	4/4
GCM:HC	4/4	4/4	4/4	4/4	4/4	4/4	4/4	4/4	4/4	4/4	4/4	4/4
GCM:PL	4/4	4/4	4/4	4/4	4/4	4/4	4/4	4/4	4/4	4/4	4/4	4/4
SSP:HC	0/4	0/4	0/4	0/4	0/4	0/4	0/4	0/4	0/4	0/4	0/4	0/4
SSP:PL	0/4	0/4	0/4	0/4	0/4	0/4	0/4	0/4	0/4	0/4	0/4	0/4
HC:PL	4/4	4/4	4/4	4/4	4/4	4/4	4/4	4/4	4/4	4/4	4/4	4/4

907

908   *Table 6. Differences in the number of drought events according to hydrological conditions*

909   (unit: occurrences)

SSPs	Basin	AD			CJ		
	Duration	3	6	12	3	6	12
245	NF	5.65	1.65	0.10	1.60	0.55	0.15
	DF	4.80	0.90	0.30	1.65	0.85	0.45
370	NF	6.25	1.65	0.45	1.60	0.20	0.55
	DF	4.35	0.90	0.25	1.85	0.55	0.30
585	NF	3.95	1.65	0.25	2.35	0.50	0.40
	DF	4.55	0.90	0.20	1.75	0.65	0.60
SSPs	Basin	HC			SJ		
	Duration	3	6	12	3	6	12
245	NF	0.40	0.25	0.10	1.45	0.60	0.15
	DF	0.45	1.25	0.85	2.00	0.30	0.10
370	NF	0.50	0.45	0.45	1.45	0.85	0.25
	DF	0.15	0.40	0.30	1.95	0.10	0.10
585	NF	0.55	0.20	0.15	2.50	0.30	0.35
	DF	0.45	0.30	0.50	1.65	0.35	0.30

910

911

912 *Table 7. Frequency of statistical significance (p < 0.05) of uncertainty sources for future*
913 *hydrological drought*

Factor	2040s	2050s	2060s	2070s	2080s	2090s
GCM	4/4	4/4	4/4	4/4	4/4	4/4
SSP	4/4	4/4	4/4	4/4	4/4	4/4
HC	4/4	4/4	4/4	4/4	4/4	4/4
PL	4/4	4/4	4/4	4/4	4/4	4/4
GCM:SSP	4/4	4/4	4/4	4/4	4/4	4/4
GCM:HC	4/4	4/4	4/4	4/4	4/4	4/4
GCM:PL	4/4	4/4	4/4	4/4	4/4	4/4
SSP:HC	0/4	0/4	0/4	0/4	0/4	0/4
SSP:PL	0/4	0/4	0/4	0/4	0/4	0/4
HC:PL	4/4	4/4	4/4	4/4	4/4	4/4

914

Table 8. Uncertainty contribution in future hydrological drought analysis from hydrological
model calibration

(unit: %)

Basins	NF	DF
AD	1.89	1.64
CJ	4.06	3.58
HC	5.56	5.27
SJ	0.26	0.26